Mokbel *et al., J. of Virol. Sci.*, Vol. 8: 12- 27, 2020
ISSN: 2636-2937

RESEARCH

Journal of Virological Sciences

Molecular Characterization of *Cucumber Mosaic Virus* and Structural Changes of Infected Sugar beet Plants

Samah A. Mokbel, Eman A. Ahmed, Hanan F. El-Kammar, Ahmed A. Kheder

ABSTRACT

Background: *Cucumber mosaic virus* (CMV) is known to occur in sugar beet plants in Egypt and may produce severe damage to infected plants. However, studies on the effect of the CMV on the cellular and internal structures of sugar beet leaves were rare.

Methods: The CMV was isolated from sugar beet samples collected during November 2018 from the Fayoum governorate, exhibited symptoms of mosaic and leaf malformation. Detection was performed depending on the presence of specific antibodies against CMV, and isolation from local lesions on *Chenopodium amaranticolor* as a local lesion host. Eleven plant species belonging to four families were used to confirm the presence of CMV in the inoculum. Detection of the coat protein gene of CMV in infected leaves has been done by reverse transcriptase-polymerase chain reaction (RT-PCR), and the appearance of 678 bp bands confirmed the expected size of such gene. Light and transmission electron microscopy were used to study the cytological and histological changes that occurred in the leaves of the sugar beet plant by the pathogen, as well as, to determine some morphometric parameters such as upper and lower epidermis thickness, midrib thickness, blade thickness, palisade tissue thickness, spongy tissue thickness, height and width of the vascular bundle.

Results: Phylogenetic analysis results indicated that SEA-CMV-isolate under study (acc. no. MT491996) closely related (99.9%) to Beet-EG-CMV-isolate (JX826591), isolated from sugar beet plants from Kafr El-Sheikh governorate, Egypt during 2012. Results of sequence analysis confirmed the classification of isolate SEA as a member of group IA. Infection of sugar beet leaves with CMV resulted in the formation of amorphous inclusion bodies in the cytoplasm. Semi thin-sections of the diseased sugar beet leaf blade showed changes in cellular organization and vascular bundles that reflect the progression of the external symptoms. Electron micrograph showed isometric spherical virus particles, measuring approximately 28 nm in diameter. Ultrathin sections showed chloroplast malformations. The malformation appeared as a chloroplast broken envelope with the presence of numerous long starch globules. Ultrathin sections revealed the virus-like particles filled the nucleus while those in chloroplast formed a distinctive crystalline shape. The shape of the cell walls and the structures of mitochondria changed under the effect of CMV in most cells.

Conclusion: The results demonstrate that the virus possesses dangerous effects that reduce the functions of the chloroplasts in sugar beet plants that may perturb the photosynthesis in chloroplasts and the synthesis of ATP in mitochondria. The results also show that the virus exerted influence on all investigated parameters. The present study provides useful information for the cytological effects and structural changes in sugar beet cells resulting from CMV infection.

Keywords: Sugar beet, *Cucumovirus*, DAS-ELISA, RT-PCR, Coat protein (CP), Sequence alignment, Inclusion bodies, Histopathology

BACKGROUND

Sugar beet (*Beta vulgaris* L. var. altissima) belongs, to and is the model species of the amaranth family (*Amaranthaceae*), represented by 175 genera and more than 2,500 species (Atanassov, 1986). Sugar beet juice contains high levels of sucrose and is second only to sugarcane as the major source of the world's sugar. In 2018, the sugar beet production in Egypt

Correspondence: samah.mokbel@arc.sci.eg
Full list of author information is available at the end of the article

was 11,222,720 tons and the cultivated area amounted to about 219087 hectares (FAOSTAT, 2019).

Cucumber mosaic virus (CMV) is the type species of the genus *Cucumovirus* in the family *Bromoviridae*. CMV is a small RNA virus capable of infecting a wide variety of plant species in 500 genera of more than 100 families (Garcia-Arenal and Palukaitis, 2008). It consists of a spherical particle of approximately 28 nm in diameter. It can be easily transmit by mechanical inoculation or aphid, more than 60 species in a non-persistent manner (Gibbs and Harrison, 1970; Francki *et al*., 1979).

The genome of CMV consists of three single-stranded RNA molecules. RNAs 1 and 2 encode components of the viral RNA-dependent RNA polymerase (RdRp), while the bicistronic RNA 3 encodes the movement protein (MP) and coat protein (CP). The nucleotide sequence of RNA-4, which contains the coat protein gene, is present in RNA-3. RNA-1 and RNA-2 are encapsidated separately and RNA-3 and the sub genomic RNA-4 are in the same particle; thus, virus preparations contain particles of at least three different types but with similar morphology. Proteins translated from RNAs 1 and 2 are associated with viral genome replication. A small overlapping gene, 2b, residing in RNA 2 and implicated in suppression of gene silencing, was discovered, expressed through a second sub-genomic RNA, and thereby this gene is also involved in symptom severity (Bujarski *et al*., 2012; Jacquemond, 2012).

Based on the genomic sequence similarity and serological relationships, CMV strains are divided into two major subgroups, subgroup I and II. Subgroup I can be further divided into two groups IA and IB (Tian *et al*., 2009; Jacquemond, 2012). Strains of CMV belonging to subgroup I induce mild green mosaic phenotype, on the other side, strains of CMV belonging to subgroup II induce a strong chlorotic phenotype (Shi *et al*., 2002; Garcia-Arenal and Palukaitis, 2008; Mochizuki and Ohki, 2012). Many of these strains are viral agents of infection in different sugar beet-growing regions in Egypt, causing severe yellowing, stunting, and vein clearing (Abdelkader *et al*., 2006; Oraby *et al*., 2008; Megahed *et al*., 2012; 2014). However, the purpose is not only to focus on the external symptoms-based largely on CMV strain but also to study the cytological and histological changes occurring in the leaves of the sugar beet plant by the pathogen.

MATERIALS AND METHODS

Plant material, serological test, and inoculation procedure

Leaves of 75 sugar beet (*Beta vulgaris* L. var. *altissima*) plants showing symptoms such as mild mosaic and pale-green mosaic areas, and malformation were collected during November 2018 from Senores center, Fayoum governorate (Fig. 1). The collected leaf samples were tested by DAS-ELISA method (Clark and Adams, 1977) using polyclonal antibody specific CMV commercial kits provided by (Agdia, USA), according to the manufacturer instructions. The single local lesions technique on *Chenopodium amaranticolor* leaves described by Kuhn (1964) was used for the biological purification of the virus. The resulting virus-isolate was propagated in *Cucurbita pepo* plants as the sources of inoculum (Francki *et al*., 1979). All biological tests were carried out by mechanical inoculation of indicator host species using the sap of homogenized *C. pepo* leaves with CMV symptoms by grinding leaf tissues with sterilized pestles and mortars in 0.1 M sodium phosphate buffer pH 7.2, at a ratio of 1:2 (tissue weight: buffer volume). The inoculated plants were observed regularly for local and systemic symptom development during 21-28 days post virus inoculation (dpi). Plants that served as negative

controls were inoculated with the buffer. The presence of CMV in host plants was further confirmed using reverse transcription-polymerase chain reaction (RT-PCR) assay.

Diagnostic hosts

A selection of eleven plant species as diagnostic hosts belonging to four families *Chenopodiaceae*, *Cucurbitaceae*, *Fabaceae*, and *Solanaceae* was included to investigate the possibility of the viral strain transmission based on symptoms development. These diagnostic hosts comprised of *Chenopodium amaranticolor*, *C. quinoa*, *Beta vulgaris*, *Cucumis sativus*, *Cucurbita moschata*, *C. pepo*, *Phaseolus vulgaris*, *Vigna unguiculata*, *Nicotiana tabacum*, *N. glutinosa*, and *Datura metel*.

Total RNA isolation and RT-PCR assay

Total RNAs were extracted from 100 mg leaves of healthy and naturally infected sugar beet, as well as mechanically inoculated plants of *Beta vulgaris*, *Cucurbita pepo*, and *N. glutinosa* (8-12 dpi) using the Geneaid RNA extraction Kit (Geneaid-Taiwan), according to the manufacturer instructions. The extracted RNA was isolated and re-suspended in 40µl of RNase-free water. RT-PCR assay was performed using CMV specific F4-forward (5′-TTGAGTCGAGTCATGGACAAATC-3′), and F3-reverse (5′-AACACGGAATCAGACTGGGAG-3′) primers of the coding region of the coat protein (CP) gene (Lin *et al*., 2004). RT-PCR was performed using reverse Verso TM one-step RT-PCR Reddy Mix Kit (Thermo scientific) in 25µl total volume containing 12.5µl of one-step PCR master mix, 5µl of nuclease-free water, 3µl of total RNA, 1.5µl (10µM) specific forward and reverse primers, 0.25µl Verso enzyme, and 1.25µl RT-Enhancer. Complementary DNA (cDNA) synthesis was done at 50°C for 15 min, 94°C for 3 min; followed by 35 cycles of 94°C at 30 sec, 50°C at 30 sec, 72°C at 2 min and a final extension for 7 min at 72°C. The 7µl of PCR products were loaded in 1.5% agarose gel prepared in TAE buffer (1x), and visualized using a UV transilluminator. The size of the amplified products was estimated using a 100 bp DNA Ladder (Biomatik).

Sequencing and phylogenetic analysis

The partial nucleotide sequence (678 nucleotides), of the Egyptian SEA-CMV-CP, was determined by an automated DNA sequencer, then compared with 26 sequences from other CMV/CP genes present in GenBank. Multiple sequence alignments and phylogenetic analyses using the maximum likelihood method with 1,000 replicate bootstrap values were performed with version MEGA X (Kumar *et al*., 2018).

Light microscopy of CMV inclusion bodies

A light microscope (OPTIKA B-350) was used to detect the inclusion bodies formed by the virus in leaves of infected plants. Epidermal strips of healthy *Beta vulgaris* and the artificially inoculated one with CMV exhibiting mosaic symptoms were removed using forceps from the underside of midribs and petioles of young leaves. The strips were dipped with a buffer solution containing 5% Triton X-100 for 10 min according to the method described by (Ahmed, 1994) and adopted by El-Banna *et al*. (2014) to facilitate the observation of the inclusion bodies, and the photographs were captured using AIPTEK-HD-DV 1080P camera.

Preparation of plant tissues for light and electron microscopy

Light and transmission electron microscopy were performed using the tissues of both healthy and inoculated fresh materials with CMV at 28 dpi. Fresh sugar beet leaves were cut into small pieces (approx. 2mm x 2 mm) in a petri dish containing 2.5% glutaraldehyde in 0.1 M Na-cacodylate buffer (pH 7.2). Following this treatment, the rinsing procedure took place in a 0.1 M solution of 0.1 M Na-cacodylate buffer for 45 minutes, with buffer changes at 15 and 30 minutes, and then fixed a second time for two hours at room temperature using 0.1 M buffer containing 1% osmium tetroxide. Following secondary fixation, the specimens were dehydrated in the ethanol series, embedded in Spurr resin as described (Rocchetta *et al*., 2007). Semi-thin sections (1mm) were cut with a glass knife, then stained with Toluidine blue for five minutes, and the sections mounted with water on glass slides. Slides were examined by OPTIKA B-350 light microscope and photographs were captured using AIPTEK-HD-DV 1080P. Different cross-sections were observed by using a microscope, images were acquired, and then the following was then measured: the thickness (µm) of the upper and lower epidermis, and the thicknesses of the different subsequent tissues (Table 3). The same blocks were then sectioned (50-nm) with a diamond knife, ultramicrotome (Leica model EM-UC6), and transferred onto 400-mesh copper grids. Sections were stained with 2% uranyl acetate and lead citrate (for 10 and 5 minutes, respectively) before examination using the JEOL electron microscope (JEM-1400 TE Japan) at the candidate magnification. Areas of interest were photographed by CCD camera model AMT, Optronics camera with 1632x1632 pixel format as side-mount configuration, at the Electron Microscope Unit, Faculty of Agriculture, Research Park, Cairo University, and (FARP).

RESULTS

Symptoms and identification of CMV

Naturally infected sugar beet-leaves with CMV exhibited symptoms of mild mosaic or pale green and darker green coloration intermixed on the leaf surface (Fig. 1). Twenty-five out of 75 naturally infected samples with CMV were identified positively using the DAS-ELISA assay as compared to the negative control. Symptoms induced mechanically with CMV on different test plants are shown in the figures (2 and 3) and summarized in Table 1. ELISA tests of all inoculated plants were all positive. Naturally infected sugar beet plants and the plants inoculated with CMV such as *Beta vulgaris*, *Cucurbita pepo*, and *Nicotiana glutinosa* were confirmed by RT-PCR using a specific pair of primers for the CP region of CMV. The RT-PCR products produced specific bands at ~ 678 bp (Fig. 4)**.**

Fig. 1: Symptoms of naturally infected sugar-beet leaves with CMV. **(A)** Mild mosaic. **(B and C)** Pale and dark green areas in the leaves.

Sequencing of PCR products and phylogenetic analysis

The 50µL amplified products of the samples were run on a 1% agarose gel and electrophoresed. Gel electrophoresis results indicated the PCR-amplified fragment was of the expected size (i.e. approximately 678 bp), as shown in Figure 4. The amplified product was cut using a sterile blade, cleaned, and sequenced. The sequenced region was submitted to GenBank under the name SEA (accession number MT491996) and included 678 nucleotides. The nucleotide sequence of SEA-CMV-isolate was compared at the nucleotide level with those of 16 CMV strains from subgroup I (A and B) and 10 strains from subgroup II. The nucleotide sequence of the examined SEA-CMV CP gene was most homologous (i.e. 99.9%) to that of the Beet-EG-CMV CP gene (accession number JX826591). The comparison revealed that isolate SEA was highly similar (99.7%) to those of previously described CMV isolates that found in different plant species in Egypt, Australia, Syria, and the USA (acc. no. JQ013954, MN259066, KT220179, KM207236, AJ296154, U22821, AB448691, D10538), as shown in Table 2. The nucleotide sequence of SEA-CMV shares more than 99% identity with those of strains in subgroup IA, and 95% identity with subgroup IB. The homology between the SEA-CMV CP gene and those of subgroup II was ranged from 78.8% to 81% (Table 2 and Figure 5).

Table (1): **External symptoms of the tested-species by inoculation of infected sap with *Cucumber mosaic virus*.**

Family	Diagnostic plant species	CMV reaction symptoms	Day
Amaranthaceae	*Chenopodium amaranticolor*	LS, CLL	4
	Chenopodium quinoa	LS, CLL	4
	Beta vulgaris	SS, MM, YM, GVB, LD	22
Cucurbitaceae	*Cucumis sativus*	SS, SM	10
	Cucurbita moschata	LS, NLL	7
	Cucurbita pepo	SS, SM	9
Fabaceae	*Phaseolus vulgaris*	LS, NLL	6
	Vigna unguiculata	LS, NLL	8
Solanaceae	*Nicotiana tabacum*	SS, SM	14
	Nicotiana glutinosa	SS, SM	10
	Datura metel	SS, M	11

CLL: Chlorotic local lesions; **NLL**: Necrotic local lesions; **LD:** Leaf distortion; **M**: Mosaic; **MM**: Mild mosaic; **SM**: Severe mosaic; **GVB**: Green veinbanding**; YM**: Yellow mosaic. **LS:** Local symptoms. **SS:** Systemic symptoms.

Fig. 2: Symptoms of the inoculated sugar beet plants with CMV. **(A and B)** The responses of plants for the mechanical inoculation, symptoms of mild mosaic, pale-green mosaic areas, and green veinbanding. **(C)** The non-inoculated plant with CMV.

Fig. 3: Symptoms of the mechanical inoculation of the CMV on some host plants. **(A)** Chlorotic local lesions in the inoculated *chenopodium amaranticolor* leaf. **(B and C)** Severe mosaic on the inoculated leaves of *Cucurbita pepo* and *Nicotiana glutinosa*, respectively. **(D and E)** Necrotic local lesions in the inoculated leaves of *C. moschata* and *Phaseolus vulgaris*, respectively.

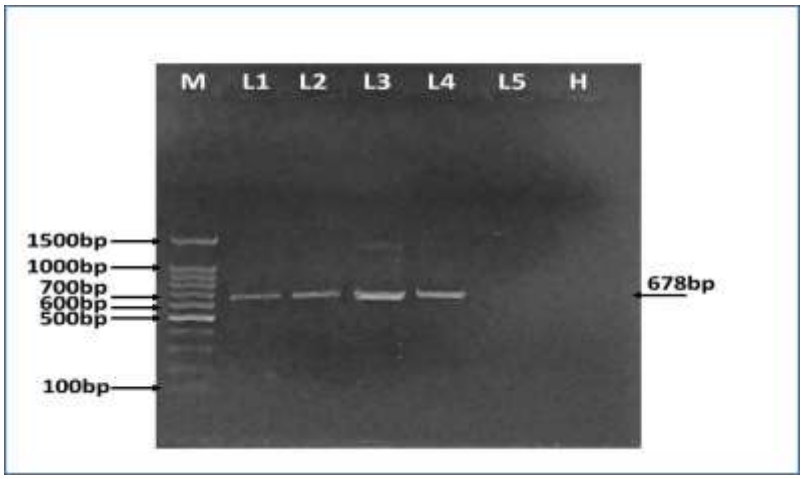

Fig. 4: Agarose gel electrophoresis patterns of RT-PCR products of *Cucumber mosaic virus*. **M**: 100 bp DNA ladder. **L1**: Sample of the naturally infected sugar beet leaves. **L2**: Sample of mechanically inoculated *Beta vulgaris* leaves. **L3**: Sample of mechanically inoculated *Cucurbita pepo* leaves. **L4**: Sample of mechanically inoculated *Nicotiana glutinosa* leaves. **L5**: Sample of non-inoculated *Beta vulgaris* leaves. **H**: Healthy plant control.

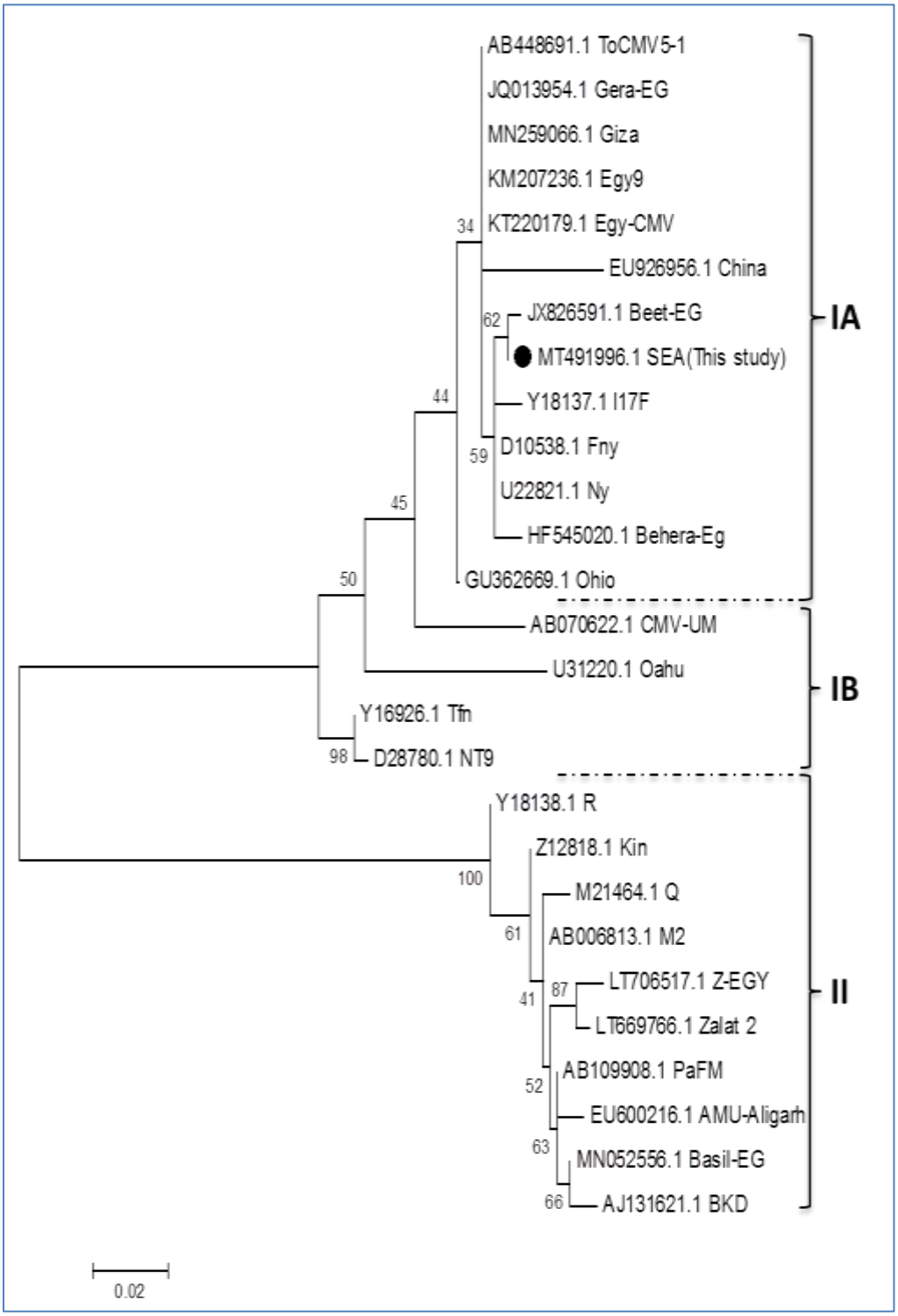

Fig. 5: The maximum likelihood tree was constructed based on available sequences of partial CP sequence of 26 CMV isolates belonging to the major subgroups I (IA, IB) and II. The phylogenetic tree of CMV was generated with the MEGA X program using bootstrap analysis with 1000 replicates and bootstrap values (≥75 %) are shown. The scale bars showed a genetic distance of 0.02.

Table (2). Comparison of the nucleotide sequences of the *Cucumber mosaic virus* (CMV) coat protein gene isolated in the present study (MT491996) with the corresponding sequences of CMV isolates from other countries.

	CMV Isolate	Accession number*	Country	Host plant	Sub-group	% Id**
1	Beet-EG	JX826591	Egypt	*Beta vulgaris*	IA	**99.9**
2	Fny	D10538	USA	NA	IA	99.7
3	Gera-EG	JQ013954	Egypt	*Geranium Pelargonium*	IA	99.7
4	Giza	MN259066	Egypt	*Cucumis sativus*	IA	99.7
5	Ny	U22821	Australia	NA	IA	99.7
6	ToCMV5-1	AB448691	Syria	*Nicotiana tabacum*	IA	99.7
7	Egy-CMV	KT220179	Egypt	*Musa* spp.	IA	99.7
8	Egy9	KM207236	Egypt	*Solanum lycopersicum*	IA	99.7
9	Ohio	GU362669	USA	*Mertensia virginica*	IA	99.0
10	I17F	Y18137	France	NA	IA	99.0
11	Behera-Eg	HF545020	Egypt	*Cucurbita pepo*	IA	99.0
12	China	EU926956	China	*Piper nigrum*	IA	96.5
13	Tfn	Y16926	Italy	*Solanum lycopersicum*	IB	95.5
14	CMV-UM	AB070622	Japan	*Prunus mume*	IB	95.2
15	NT9	D28780	Taiwan	NA	IB	95.2
16	Oahu	U31220	USA	*Musa* spp.	IB	93.4
17	R	Y18138	France	NA	II	81.0
18	Q	M21464	Australia	NA	II	80.6
19	M2	AB006813	Japan	NA	II	80.3
20	Kin	Z12818	Scotland	NA	II	80.3
21	PaFM	AB109908	Korea	*Capsicum annuum*	II	80.3
21	Basil-EG	MN052556	Egypt	*Ocimum basilicum*	II	79.9
23	Zalat 2	LT669766	Egypt	NA	II	79.6
24	AMU	EU600216	India	*Ocimum sanctum*	II	79.6
25	BKD	AJ131621	Netherland	NA	II	79.2
26	Z-EGY	LT706517	Egypt	*Nicotiana glauc*	II	78.8

*CMV-isolates can be directly queried with any protein sequence in the GenBank database by accession number pressing. **Id: Identity and the highest identity value indicated in bold. NA: Not available.

Light microscopy of CMV Inclusions

The light microscope of the epidermal strip from the lower surface of CMV infected sugar beet leaf showed amorphous cytoplasmic inclusion bodies attached to the nucleus from one or two sites, while these inclusions were not observed in the epidermal stripe of healthy leaves (Fig. 6).

Anatomical and ultrastructural changes in plant tissues

Infection with CMV affected the upper and lower layers of the epidermis, the cellular organization of the tissues, and the arrangement of vascular bundles in sugar beet leaves, as shown in Figure (7 and Table 3). Anatomy of the diseased leaf blade showed two sides of different thickness, characterized by narrow spaces with a reduction of thickness by 21.21% and 25.21% than those of healthy leaf blade. The midrib thickness was reduced by 33% in the infected leaf compared to a healthy one. Most of the palisade cells in the mesophyll tissue lost their columnar shape due to the disintegration of their cell wall. The palisade parenchyma with a thickness of 29.9 µm was small in comparison with spongy parenchyma. The center of the cross-section revealed compacted vascular bundles, which appeared as an incomplete circular shape

that linked to the change of their dimensions (height and width by 51.23% and 44.85%, respectively).

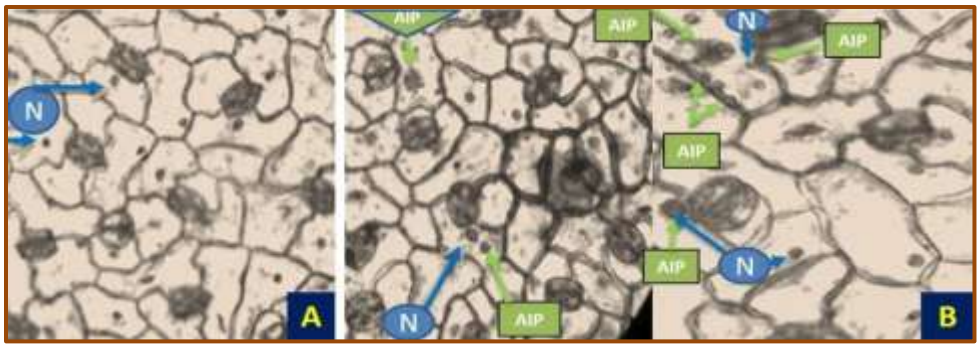

Fig. 6: The CMV inclusion bodies under 100-x magnification of light microscope. **(A)** Inclusion bodies were not present in the epidermal strip of healthy sugar beet leaf. **(B)** Amorphous inclusion bodies (AIP) present in the epidermal strip of infected leaf with CMV 28 days post-inoculation. **N,** Nucleus.

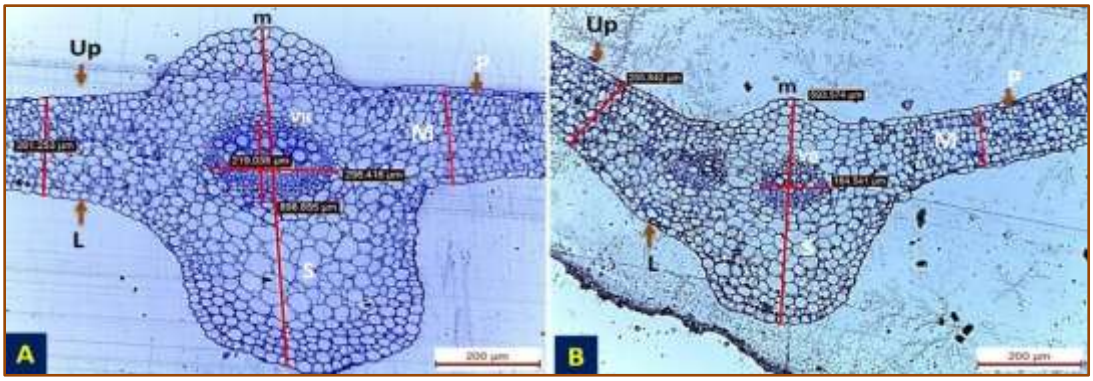

Fig. 7: Cross-sections of leaves of healthy and inoculated sugar beet by CMV. **(A)** Healthy anatomical structure. (**B)** The anatomical structure of inoculated leaf with CMV 28 days post-infection. **L**, Lower epidermis; **M**, Mesophyll; **m,** Midrib**; P,** Palisade cells; **S**, Spongy tissue; **Up**, Upper epidermis; **VB**, Vascular bundle.

Table (3): The variations in the anatomical parameters of leaves of healthy and inoculated sugar beet infected by CMV.

Plant parameters (µm)	Healthy sample	Inoculated sample	Change Percentage (%)
Upper epidermis thickness	15.440	17.700	+14.64
Lower epidermis thickness	18.760	16.400	-12.58
Midrib thickness	896.65	593.57	- 33.80
Blade thickness (Left)	261.25	205.84	-21.21
Blade thickness (Right)	261.25	195.37	-25.21
Palisade tissue thickness	64.650	29.920	-53.72
Spongy tissue thickness	105.12	93.120	-11.42
Vascular bundle height	219.03	106.80	-51.23
Vascular bundle width	298.40	164.54	-44.85
Protoxylem vessels height	28.850	17.140	-40.58
Protoxylem vessels width	26.910	20.360	-24.34
Metaxylem vessels height	42.800	18.720	-56.26
Metaxylem vessels width	26.690	20.480	-23.26

Under the Transmission electron microscope, chloroplasts infected with CMV were quite variable in shapes such as crescent shape and small circular form (Fig. 8A), and their location was quite also different, besides the shrinkage of outer and inner membranes of the chloroplasts with a break occurred in the internal part of the chloroplast (Fig. 8B). The most chloroplasts contained disorganizing grana aggregates, but the others have no grana stacks in the interior structures. These chloroplasts did not connect by large starch grains (Figs. 8A and B). Figure 9 showed the destruction of chloroplasts with enlarged starch grains that had various structures such as oval or ellipse shapes, with the disappearance of the thylakoid stacks. Structural abnormalities of mitochondria with degenerated inner membranes observed in every cell, finally the cells appeared almost devoid of organelles or fully lysed. Figures 10A and B showed that the cell walls of infected cells with CMV had irregular patterns or were malformed in shape. The virus particles were isometric, approximately 28 nm in diameter (Figs.10C and D), and were attached to cell walls or scattered around them (Fig.10E). However, most of these particles were invaded the cell wall (Fig.10B) or placed perpendicular to the outer membrane of the chloroplast (Fig.10E), and many of these particles were found in the nucleus (Figs. 9 and 10F). An arrangement of CMV particles inside the chloroplast formed a distinctive crystalline shape, as shown in Figure 10G. In contrast, cell walls, chloroplasts, and mitochondria in the healthy cell exhibit quite specific morphologies (Fig. 10H).

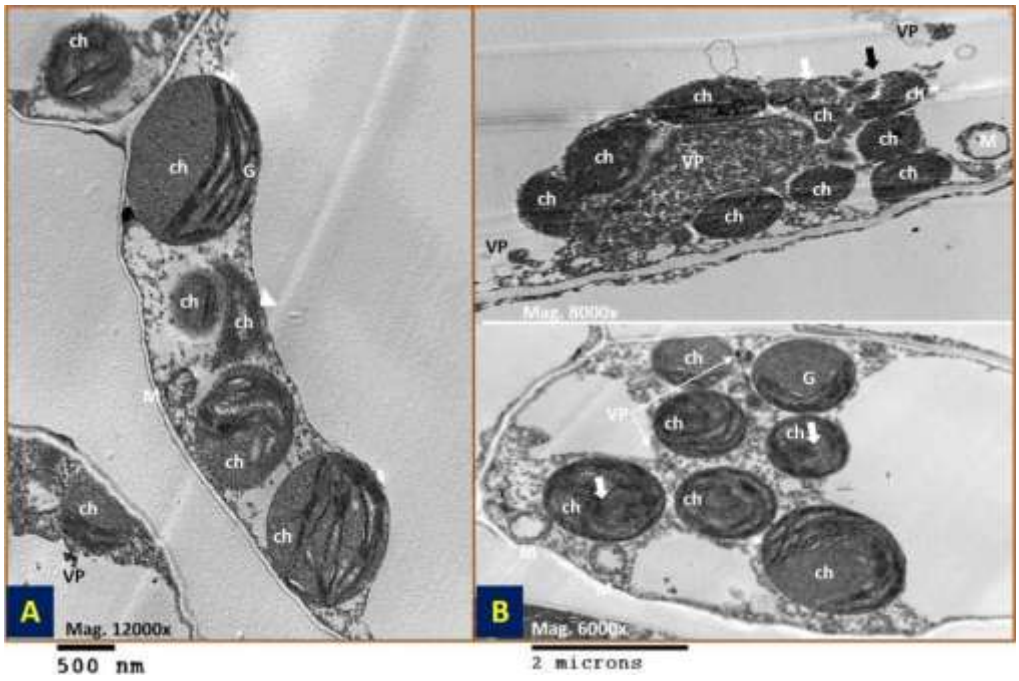

Fig. 8: Ultrastructure of the changed chloroplasts of *Beta vulgaris* by a CMV infection after 28 days post-inoculation. **(A)** An electron micrograph reveals irregular shapes of chloroplasts such as crescent and a small circular shape (the arrowhead). **(B)** An electron micrograph that shows the shrinkage of the outer and inner membranes of the chloroplasts, the collapse of the inner part of the chloroplasts (the black arrow), the disorganized grana stacks in the chloroplasts (white arrows), and the mitochondrial disorder (M) with the inner membranes degraded or lysed due to a viral infection. **Ch,** Chloroplast; **G**, Grana; **M**, Mitochondria**; VP,** Virus-like particles.

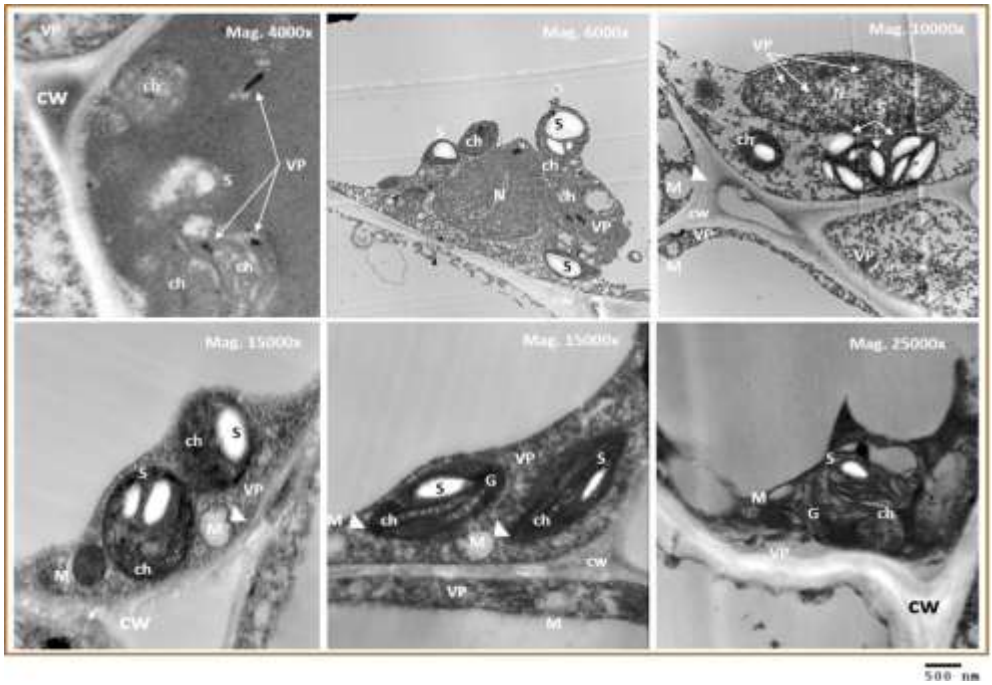

Fig. 9: Ultrastructure changes in leaf chloroplasts with starch granules. TEM micrographs showing the deformed chloroplast with unusual starch granules distributions and various forms of chloroplast such as oval or ellipse shape, the collapse of the thylakoid stacks, the dense accumulation of virus-like particles in the nucleus, and the completely degradative mitochondria (the arrowheads) by a CMV infection. **CW,** Cell wall; **Ch,** Chloroplast; **G**, Grana**; M**, Mitochondria**; N,** Nucleus**; VP,** Virus-like particles; **S**, Starch.

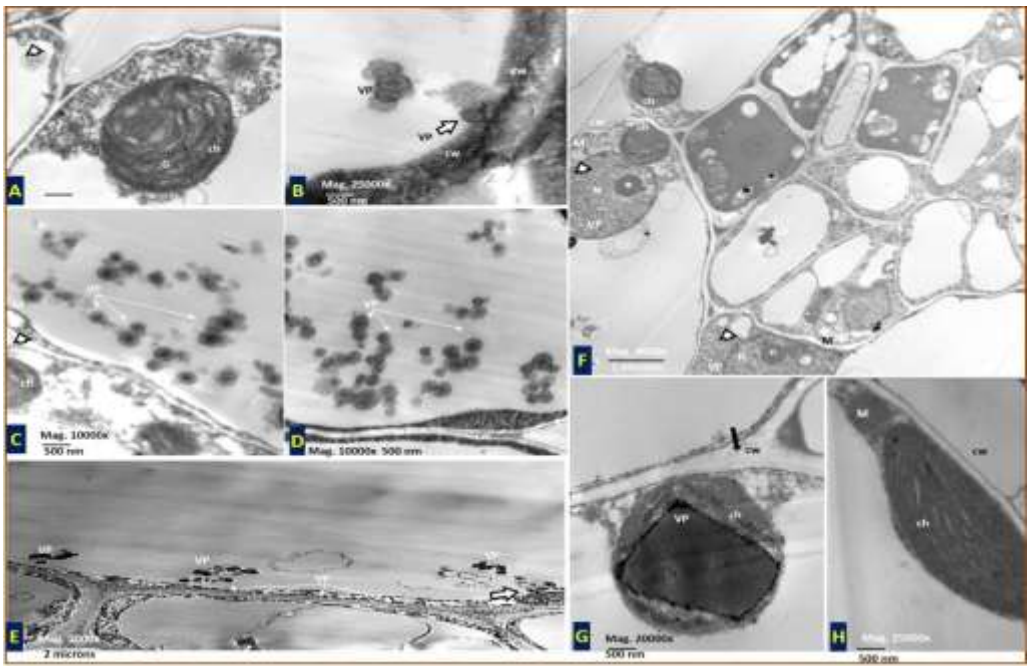

Fig. 10: TEM micrographs revealing the deformed cell walls by a CMV infection and the presence of invasive virus particles **(A and B)**. The spherical shape of virus particles with a diameter of 28 nm **(C and D)**. The presence of numerous virus particles attached

to cell walls, or scattered around them **(E)**. The mitochondria cell lysis (the arrowheads) and the dense accumulation of virus-like particles in the nucleus **(F)**. Viral particles were aggregated in crystalline rows into the chloroplast and forming crystals bodies **(G)**. Regular shapes of cell wall, chloroplast, and mitochondria of healthy leaf cells **(H)**. White arrows indicate the site of the perpendicular virus particle to the outer membrane of the chloroplast while a black arrow refers to the uneven thickening of the cell wall, **CW,** Cell wall**; Ch,** Chloroplast; **G,** Grana; **M**, Mitochondria**; N,** Nucleus; **VP,** Virus particles.

DISCUSSION

Cucumber mosaic virus (CMV) is one of the most destructive viruses and affecting the sustainability of crops in countries of the Mediterranean basin (Gallitelli, 2000; Jacquemond, 2012). In this study, DAS-ELISA assay using anti-CMV polyclonal antibody revealed the presence of virus infections in 33.3% (25 out of 75) symptomatic sugar beet leaf tissue samples, that showing mild mosaic and leaf malformation, collected from the Fayoum governorate in Egypt. During virus transmission tests, the causal virus was successfully transmitted by mechanical inoculations to many test species; the obtained results (Summarized in Table 1) are very much in line with results from other investigations (Sofy and Soliman, 2011; Megahed *et al*., 2012; Kim *et al*., 2014). The developed systemic mosaic symptoms on *Cucumis sativus* also indicating that the causative virus is an isolate of CMV since *C. sativus* is a well-known diagnostic host for CMV (Gibbs and Harrison, 1970; Francki *et al*., 1979). Besides, the isolate caused the mild green mosaic symptoms on the inoculated sugar beet with CMV with an agreement with previous reports concerning phenotype symptoms induced by CMV subgroup I strain, not the clarity-phenotype by subgroup II (Shi *et al*., 2002; Garcia-Arenal and Palukaitis, 2008; Mochizuki and Ohki, 2012). This type of phenotype corresponds, completely, to that described in the literature as being characteristic of the CMV infection associated with size-reduced chloroplasts containing fewer grana (Roberts and Wood, 1982). Also, during TEM examinations, spherical particles ~28 nm in diameter were observed, which is a characteristic feature of CMV as described by Francki *et al*. (1979), and similar to those reported for CMV isolate of sugar beet plants (Megahed *et al*., 2014). Furthermore, identification of CMV was confirmed through molecular characterization of the virus infecting sugar beet. Gel electrophoresis results indicated the PCR-amplified fragment was of the expected size (Approximately 678 bp) using specific primer pair according to Lin *et al*. (2004). The isolate SEA showed the highest similarity (99.9%) to the sequence of isolate Beet-EG and 99.7 to the sequence of isolates Fny, Gera-EG, Giza, Ny, ToCMV, Egy-CMV, and Egy9 (subgroup IA). While, the same isolate showed 79.9%, 79.6%, and 78.8% in nucleotide identity with the Basil-EG, Zalat 2, and Z-EGY strains (subgroup II) respectively. The SEA-CMV-isolate showed similar nucleotide identity, with several isolates (subgroup IA) in and outside of Egypt, which showing its mixed origin and makes it more stable in this type of environment. Phylogenetic tree based on the CP gene sequence revealed the presence of isolate SEA, in the current study, in subgroup I, supported by 1000 bootstrap value. Moreover, most of the previously described Egyptian CMV isolates classified into group I based on and nucleotide sequence identity, regardless of infected plant type. In this regard, Fraile *et al*. (1997) suggest that the naturally infected crops with strains of sub-group (I), which described as a sub-group (heat-resistant), are more frequent than strains of a subgroup (II) and represent more than 80% of all isolates. This means that CMV subgroup (I) strains generally induce more severe disease than those of subgroup II (Hord *et al*., 2001; Tian *et al*., 2009; Jacquemond, 2012). Accordingly, the infected

plants with strains of sub-group (I) are considered the main sources of the virus movement and spreading.

Anatomical changes showed that the thickness of the leaf blade and midrib, the thickness of the lower epidermis, the thickness of palisade and spongy cells, as well as the dimension of the vascular bundles, were decreased in the infected plant as compared to healthy. In the available literature, there are no exact numerical indicators about the impact of CMV on the mentioned parameters of sugar beet plants (Table 3). However, many authors confirmed that the reduction in palisade tissue thickness, mesophyll thickness, and area of both upper and lower epidermis cells from two tomato species occurs in response to CMV (isolate 746-07) (Janjic and Eric, 2012). Afreen *et al*. (2010) also reported that the thickness of the xylem zone in the midrib region of the leaf reduced in the infected *Daucus carota* with CMV. Kunkalikar *et al*. (2007) and El-Attar *et al*. (2019) reported similar observations in infected papaya and basil leaves with the *Papaya ringspot virus* and the *Alfalfa mosaic virus*, which showed an irregular both palisade and spongy cells.

In terms of the CMV-influence on sugar beet cells, the structural organization, the disorder of mitochondria, and a high dissociation of chloroplast envelopes observed after CMV infection. These changes mean that CMV reduced the functions of the chloroplasts in the infected plants thus disturbed the synthesis of mitochondrial ATP synthase, and the overall catalytic mechanism of the chloroplast ATP synthase (Song *et al*., 2009). The present study also observed compared with healthy sugar beet-leaves the presence of unusual photosynthetic structures such as the disappearance of grana stacks, or distorted thylakoid, and the destroyed chloroplasts. It is suggested that modification of photosynthesis is a strategic mechanism for virus pathogenesis to facilitate infection and virus movement or to establish productive infection or replication within the host (Gunasinghe and Berger, 1991). Besides, the evidence of crystalline inclusion bodies in the chloroplasts, and amorphous inclusion bodies in the cytoplasm, or virus-like particles in other locations like nucleoli and mitochondria, suggest that further direct invasion of CMV from infected cells to neighboring cells, accordingly, the virus can replicate in these cells. Matthews (1991) found that the changes that appeared in chloroplasts and nucleoli might support the replication of the virus and its possible movement in these tissues. According to Fogh (1961) and Esau *et al*. (1966), the occurrence of crystalline arrays or rows is a "physical phenomenon" associated with the high concentration of virus particles. Thus, the present study indicates that the virus affects all examined plant tissues so one may conclude that sugar beet productive ability may decrease soon.

CONCLUSION

The alignment based on a MEGA X program with all available CMV sequences confirmed that SEA is an isolate of CMV (acc. no. MT491996). The CMV found scattered in different areas and appears as amorphous inclusion bodies in the cytoplasm, as crystalline inclusion bodies in the chloroplasts, and as virus-like particles in the mitochondria and the nucleus. The SEA-CMV-isolate multiplied in different parts of the cell, which can severely affect the yield and quality of sugar beet.

AUTHOR DETAILS

Virus and Phytoplasma Research Department, Plant Pathology Research Institute. Agricultural Research Center ARC, P.O. Box 12619, Giza, Egypt.

RECEIVED: May, 2020; **ACCEPTED**: June 2020; **PUBLISHED:** July 2020

REFERENCES

Abdelkader, H.S., Khatab, E.H., and Abd El Fattah, A.I. (2006). Detection and identification of an Egyptian isolate of *Cucumber mosaic virus* (CMV) affecting Sugarbeet using non-radioactive RNA probe. Pak. J. Biotechnol., 3(1-2) 1-10.

Afreen, B., Baghel, G., Fatma, M., Usman, M., and Naqvi, Q.A. (2010). Studies on molecular detection of *Cucumber mosaic virus* and its anatomical and biochemical changes in *Daucus carota* L. Int. J. Gen. Eng. Biotechnol., 1(3):187-192.

Ahmed, A.A. (1994). Studies on viral diseases of stone-fruits. M.Sc. Thesis, Plant Pathology Department, Faculty of Agriculture, Ain Shams University. 125 pp.

Atanassov, A.I. (1986). Sugar Beet (*Beta vulgaris* L.). In: Bajaj Y.P.S. (eds) Crops I. Biotechnology in Agriculture and Forestry, vol 2. Springer, Berlin, Heidelberg.

Ausubel, F.M., Brent, R., Kingston, R.E., Moore, D.D., Seidman, J.G., Smith, J.A., and Struhl, K. (1989). Current protocols in molecular biology. John Wiley and Sons, New York.

Bujarski, J., Figlerowicz, M., Gallitelli, D., Roossinck, M.J., and Scott, S.W. (2012). *Bromoviridae*. In Virus Taxonomy: Classification and Nomenclature of Viruses: Ninth Report of the International Committee on Taxonomy of Viruses, pp. 965-976. Edited by A.M.O. King, M.J. Adams, E.B. Carstens, and E.J. Lefkowitz. London, UK: Elsevier.

Clark, M.F., and Adams, A.N. (1977). Characteristics of the microplate method of enzyme linked immunosorbent assay for the detection of plant viruses. J. Gen. Virol., 34: 475-483.

El-Attar, A.K., Mokbel, A.S. and El-Banna, Om-Hashem M. (2019). Molecular characterization of *Alfalfa Mosaic Virus* and its effect on Basil (*Ocimum basilicum*) tissues in Egypt. J. Virol. Sci., 5:97-113.

El-Banna, Om-Hashem M., Awad, M.A.E., Abbas, M.S., Waziri, H.M.A., and Darwish, H.S.A. (2014). Anatomical and ultrastructural changes in tomato and grapevine leaf tissues infected with *Tomato ringspot nepovirus*. Egypt. J. Virol., 11(2):102-111.

Esau, K., Cronshaw, J., and Hoefert, L.L. (1966). Organization of *Beet yellows-virus* inclusions in leaf cells of *beta*. PROC.N.A.S., 55(3): 486-493.

FAOSTAT, (2019). The data set "Sugar beet, production quantity (Tons)", and Area harvested (Hectare), for Egypt contains data from the year 1961 until 2018. http://www.fao.org/faostat/en/?#data/QC

Fogh, J. (1961). Filamentous organization of poliovirus particles. J. Virol., 14: 495-497.

Fraile, A., Alonso-Prados, J.L., Aranda, M.A., Bernal, J.J., Malpica, J.M., and Garci-Arenal, F. (1997). Genetic exchange by recombination or re-assortment is infrequent in natural populations of a tripartite RNA plant virus. J. Virol., 71: 934-940.

Francki, R.I.B., Mossop, D.W., and Hatta, T. (1979). *Cucumber mosaic virus*. CMI/AAB Descriptions of Plant Viruses No. 213. http://www.dpvweb.net/dpv/showadpv.php?dpvno=213

Gallitelli, D. (2000). The ecology of the *Cucumber mosaic virus* and sustainable agriculture. Virus Res., 71(1-2): 9-21.

Garcia-Arenal, F. and Palukaitis, P. (2008). *Cucumber mosaic virus*. In: Mahy B.W.J., van Regenmortel M.H.V. (eds). Encyclopedia of Virology, 3rd Ed., Elsevier-Academic Press, San Diego, CA, USA. pp. 614-619.

Gibbs, A.J., and Harrison, B. D. (1970). *Cucumber mosaic virus*. CMI/AAB Descriptions of Plant Viruses No. 1. http://www.dpvweb.net/dpv/showadpv.php?dpvno=1

Gunasinghe, U., and Berger, P. (1991). Association of *Potato virus Y* gene products with chloroplasts in tobacco. Mol. Plant. Microbe Interact., 4: 452-457.

Hord, M.J., Garcı´a, A., Villalobos, H., Rivera, C., and Macaya, G. (2001). Field surveys of *Cucumber mosaic virus* subgroups I and II in crop plants in Costa Rica. Plant Dis., 85: 952-954.

Jacquemond, M. (2012). *Cucumber Mosaic Virus*. Adv. Virus Res., 84: 439-504.

Janjic, N., and Eric, Z. (2012). Morphometric and anatomical-histometric characteristics of two varieties of the species *Solanum lycopersicum* L. infected by *Cucumber mosaic virus*. Agroznanje, 13(4): 591-602.

Kim, M.K., Jeong, R.D., Kwak, H.R., Lee, S.H., Kim, J.S., Kim, K.H., Cha, B., and Choi, H.S. (2014). First Report of *Cucumber mosaic virus* Isolated from Wild *Vigna angularis* var. *nipponensis* in Korea. Plant Pathol. J., 30(2): 200-207.

Kuhn, C.W. (1964). Separation of *Cowpea virus* mixture. Phytopathol., 54: 739-740.

Kumar, S., Stecher, G., Li, M., Knyaz, C., and Tamura, K. (2018). MEGA X: Molecular evolutionary genetics analysis across computing platforms. Mol. Biol. Evol., 35(6): 1547-1549.

Kunkalikar, S., Byadgi, A.S., Kulkarni, V.R., Krishnareddy, M., and Prabhakar, A.S.N. (2007). Histopathology and histochemistry of papaya ringspot disease in papaya. Indian J. Virol., 18(1): 33-35.

Lin, H.X., Rubio, L., Smythe, A.B., and Falk, B.W. (2004). Molecular population genetics of *Cucumber mosaic virus* in California: evidence for founder effects and reassortment. J. Virol., 78(12): 6666-6675.

Matthews, R.E.F. (1991). Plant virology. 3rd Edn., Academic Press, San Diego, Pages: 835.

Megahed, A.A., El-Dougdoug, K.A., Othman, B.A., Lashin, S.M., Ibrahim, M.A., and Sofy, A.R. (2012). A new Egyptian satellite strain of *Cucumber mosaic cucumovirus*. Int. J. Virol., 8: 240-257.

Megahed, A.A., El-Dougdoug, Kh.A., Othman, B.A., Lashin, S.M., Hassanin, M.D., Ibrahim, M.A., and Sofy, A.R. (2014). Molecular identification and analysis of coat protein gene of *Cucumber mosaic cucumovirus* sugar beet Egyptian isolate. Int. J. Plant Pathol., 5: 70-83.

Mochizuki, T., and Ohki, S.T. (2012). *Cucumber mosaic virus*: viral genes as virulence determinants. Mol. Plant Pathol., 13(3): 217-225.

Oraby, M.M., El-Borollosy, A.M., and Abdel Ghaffar, M.H. (2008). Molecular characterization of a "Sugar beet" *Cucumber mosaic cucumovirus* isolate and its control via some plant growth-promoting rhizobacteria. J. Biol. Chem. Environ. Sci., 3: 147-167.

Roberts, P.L., and Wood, K.R. (1982). Effects of a severe (P6) and a mild (W) strain of *Cucumber mosaic virus* on tobacco leaf chlorophyll, starch and cell ultrastructure. Physiol. Plant Pathol., 21: 31-37.

Rocchetta, I., Leonard, P.I., and Filho, G.M.A. (2007). Ultrastructure and X-ray microanalysis of *Euglena gracilis* (Euglenophyta) under chromium stress. Phycologia, 46(3):300-306.

Shi, B.J., Palukaitis, P., and Symons, R.H. (2002). Differential virulence by strains of *Cucumber mosaic virus* is mediated by the 2b gene. Mol. Plant Microbe Interact., 15(9): 947-955.

Sofy, A.R., and Soliman, A.M. (2011). Molecular identification of a *Cucumber mosaic virus* subgroup I Egyptian isolate from geranium based on bioinformatics analysis of CP gene sequence. Egypt. J. Virol., 8: 178-194.

Song, H.S., Wang, Y.J., Mao, W.H., Shi, K., Zhou, Y.H., Nogues, S., and Yu, J.Q. (2009). Effects of *Cucumber mosaic virus* infection on electron transport and antioxidant system in chloroplasts and mitochondria of cucumber and tomato leaves. Physiol. Planta., 135: 246-257.

Tian, Z., Qiu, J., Yu, J., Han, C., and Liu, W. (2009). Competition between *Cucumber mosaic virus* subgroup I and II isolates in tobacco. Phytopathol. J., 157: 457-464.

Cite this article as:
Mokbel ***et al.,*** **(2020):** Molecular Characterization of Cucumber Mosaic Virus and Structural Changes of Infected Sugar beet Plants. *Journal of Virological Sciences*, Vol. 8: 12- 27.